Hindawi
Advances in Civil Engineering
Volume 2018, Article ID 9473947, 13 pages
https://doi.org/10.1155/2018/9473947

Research Article

Mechanical Properties of Grouted Crushed Coal with Different Grain Size Mixtures under Triaxial Compression

Yuhao Jin,[1,2] **Lijun Han**,[1] **Qingbin Meng**,[1] **Suresh Sanda**,[3] **Haizhi Zang**,[1,2,4] **and Bing Feng**[1]

[1]*State Key Laboratory for Geomechanics and Deep Underground Engineering, School of Mechanics and Civil Engineering, China University of Mining and Technology, Xuzhou, Jiangsu 221116, China*
[2]*State Key Laboratory of Coal Resources and Safe Mining, China University of Mining and Technology, Xuzhou, Jiangsu 221116, China*
[3]*Full Bright Consultancy (Pvt.) Ltd., 316 Baburam Acharya Sadak, Kathmandu 44600, Nepal*
[4]*School of Resources and Safety Engineering, Central South University, Changsha, Hunan 410083, China*

Correspondence should be addressed to Lijun Han; hanlj@cumt.edu.cn

Received 9 January 2018; Accepted 26 March 2018; Published 13 August 2018

Academic Editor: Yan Peng

To have a better understanding of the reinforcement effect on the crushed zone after grouting in coal mining extraction work, a self-designed grouting apparatus was used to study the effects of the grain size mixtures (distribution) and the stress state on the mechanical behaviours of grouted crushed coal specimens. From the various grouting tests, triaxial compression tests and scanning electron microscopy (SEM) observations of grouted specimens with different grain size mixtures, it was found that, for the same grain size mixture, the peak (σ_p) and residual (σ_r) strengths of the grouted specimens increased with an increase in confining pressure. It was found that the average slope values of the σ_p-σ_3 curves for the grouted specimens with different grain size mixtures were all larger than those of the σ_r-σ_3 curves. It was observed that the peak strain (ε_p) of the grouted specimens with different grain size mixtures increased overall with increasing confining pressure. For constant confining pressure, the peak and residual strengths both gradually increased approximately linearly as the grain size mixtures varied from small to large, but at higher confining pressures, the influence of the grain size mixture on the peak (or residual) strength increased. These mechanical behaviours of the grouted crushed coal specimens were strongly dependent on the variation in the grain size mixtures and in the confining pressure, which can be explained by the crack evolution process within the grouted specimen under triaxial compression, to a certain extent. Ultimate failure of the grouted specimen occurred just after propagation and coalescence of the cracks through the entire grouted specimen. Moreover, there were three major microscopic diffusion modes for the grouts flowing in most of the crushed coal specimens. Based on these test results, it was found that the reinforcement effect of the grouted specimen related to the splitting grouting mode (occurring in most of the large specimens) seems to be better than that of the penetrating (filling) grouting mode (in most of the small specimens).

1. Introduction

Coal exploration work is mostly invasive and causes strata fracture, which could consequently result in significant interface subsidence, water loss, cracks, and even partial fragmentation (eventually forming the crushed zone). Different grain size mixtures are randomly distributed within the coal roof, wall, and pillar of a coal seam in the western China mining area where the overlying rock structures for most of the main coal seams are typically at shallow depths and are overlaid by thick sand layers and underlaid by thin bedrock, which poses substantial safety issues for mining operations. Grouting is a technique that can effectively improve the physical and mechanical characteristics of the fractured rock, including the crushed zone with many crack openings and voids (e.g., the abovementioned partial fragmentation), which has been widely applied in geotechnical and mining engineering [1–6]. The grouting technique can achieve the main objective of rock mass reinforcement by injecting, filling (even splitting grouting), conglutinating,

and solidifying the rock mass, successively. To have a better understanding of this consolidating technique for rock and soil materials with low strengths due to various defects (e.g., cracks and voids), many experimental and numerical studies have been performed in recent decades [7–9]. These abovementioned studies mainly concentrated on the grouting mechanism of the fractured rock, that is, the patterns of grout propagation through the rock cracks, diffusion radius of grouts in fractured rock, and grout flow through the fracture network within the rock mass which is similar to the flow of fluid (or gas) in fractured rock [10–12], but it is rare to find reports on how grouting improves the mechanical characteristics of fractured rock, much less than that of the crushed rock mass. Shu et al. [13] numerically studied the variation in the mechanical behaviours of fractured rock before and after grouting, considering the heterogeneity of the components in the grouted specimen (e.g., rock particles, grout properties, and some random microcracks within the rock). Although the numerical study has yielded some useful results, there are still many gaps and very few studies on the mechanical behaviours of fractured rock after grouting by means of the experimental approach, and there are even fewer studies on crushed rock due to the difficulty of crushed rock sampling from actual underground engineering sites, as well as the inconvenience of recreating and testing crushed rock specimens in the laboratory due to their broken characteristics [14]. Hence, the mechanical behaviours of grouted crushed coal are a key issue in this study, which may be affected by many factors, such as grouting quantity, grain size distribution (grain size mixtures), and geological stress state.

Historically, to determine the influence of flow on the grain size ratios and consequently on the hydraulic properties of the grain mixtures, many researchers have investigated water flow through noncemented media (e.g., in dam filter layers). Moreover, several experimental studies have been reported in the literature on the investigation of hydraulic properties due to water flux in noncemented crushed coal specimens and other noncompacted sedimentary rocks [15–18]. For noncemented coal particles, many theoretical, experimental, and numerical methods have been performed to investigate the effects of properties such as grain size, density, and ash on fixed characteristics. Permeability was influenced by the grain size distribution, fracture geometry [19], and water content [12]. In the study conducted by Ma et al. [20], the evolution of permeability within crushed rocks under water flow was experimentally investigated. In these studies, the seepage characteristics of water flow through the grain mixtures were discussed. However, there are very few experimental investigations on the grouts flowing through rock grain mixtures and the mechanical behaviours of the grain mixtures after grouting. The purpose of this study is to experimentally investigate the influence of varying particle size mixtures and stress conditions (axial and confining pressures) on the mechanical properties of grouted crushed coal. In this paper, the test specimens of crushed coal and the grouting material are presented first in Specimen and Grout Preparation. In addition, Testing System introduces a self-designed grout testing system, and the detailed experimental procedure and methods are described in Experimental Procedure and Methods. The experimental study on the mechanical behaviours, crack evolution mechanism, ultimate failure features, and microscopic cementation features based on the major microscopic diffusion modes of grouts in the grouted crushed coal is given in the next sections. Finally, the last section concludes and discusses the implications of these findings.

2. Test Material and Equipment

2.1. Specimen and Grout Preparation. The grain size of underground crushed coal is largely variable [20]. The experimental cylindrical grouting inner barrel had a diameter of 270 mm and a height of 500 mm (additional details are provided in the next section); the coal was broken into 4.75–37.5 mm diameter specimens; and then, the different sizes of the coal gravels were mixed to obtain different grain size distributions in the crushed coal specimens. The coal specimens used in this study were from Zhaozhuang mine, Shanxi province, China, with an average dry density of 1276 kg/m^3, characterized by higher brittleness and lower elastic modulus, crushability, and compressibility compared with those of the harder rocks (e.g., granite, quartzite, and marble). In coal mining extraction work, due to the crushability and compressibility of the coal mass, the crushed coal gravel easily occurs within the coal roof, wall, and pillar. The coal specimens in the laboratory were broken into smaller particles that were less than 37.5 mm. Using different sieve sizes, the crushed coal gravels were graded into six groups with different grain size ranges, namely, 4.75–9.5 mm, 9.5–16 mm, 16–19 mm, 19–26.5 mm, 26.5–31.5 mm, and 31.5–37.5 mm (Table 1). To investigate the impact of particle transfer on the permeability of crushed mudstones, as per [21], the tests were conducted with different grain size mixtures but the same initial porosity. In our study, coal mixtures with small differences in the initial porosity to avoid the impact of porosity as much as possible were prepared and designed. Based on these porosities of different grain sizes (Table 1), we mixed samples of different grain sizes and obtained several groups of grain size mixtures with similar porosity after multiple mixing tests (Table 2). For the simplicity of referencing in this paper, the abovementioned mixed test specimens are referred to as "small specimen," "medium specimen," and "large specimen," which are the relative concepts and represent the "grouted specimen with small grain size mixtures," "grouted specimen with medium grain size mixtures," and "grouted specimen with large grain size mixtures," respectively. An example of the medium crushed coal specimen is shown in Figure 1.

To find an appropriate water-cement ratio of the grouts (ordinary Portland cement (OPC) grouts), the study of the effect of different water-cement ratios on the flow and mechanical properties of the grouts was carried out by using the digital viscometer and AEC-201 cement strength testing machine in the laboratory. The experimental results of the viscosity and the strength of the grouts after 28 days of curing are shown in Figure 2, which reflect the rheological and mechanical properties of the grouts. Based on

Table 1: The porosity of crushed coal with different grain sizes.

Grain size (mm)	Density	First measurement		Second measurement		Third measurement		Porosity
		Volume (cm^3)	Quality (g)	Volume (cm^3)	Quality (g)	Volume (cm^3)	Quality (g)	
4.75–9.50	1.276	4000	2591	4000	2753	4000	2663	0.477
9.50–16.0	1.276	4000	2583	4000	2675	4000	2521	0.492
16.0–19.0	1.276	4000	2517	4000	2616	4000	2583	0.496
19.0–26.5	1.276	4000	2512	4000	2554	4000	2620	0.498
26.5–31.5	1.276	4000	2443	4000	2536	4000	2494	0.512
31.5–37.5	1.276	4000	2435	4000	2312	4000	2372	0.535

Table 2: Grouted specimens with different grain size distributions used in this research.

Grouted coal-crushed body	Grouted specimens with different confining pressure	Volume ratio to different grain size	Grain size mixtures	Similar initial porosity	Type of test
A1	A1-0; A1-5; A1-10; A1-15; A1-20	9.5–16 mm : 19–26.5 mm = 1 : 3	Small	0.4967	Triaxial
A2	A2-0; A2-5; A2-10; A2-15; A2-20	9.5–16 mm : 19–26.5 mm = 1 : 3	Small	0.4967	Triaxial
A3	A3-0; A3-5; A3-10; A3-15; A3-20	9.5–16 mm : 19–26.5 mm = 1 : 3	Small	0.4967	Triaxial
A4	The test specimens chosen from A4	9.5–16 mm : 19–26.5 mm = 1 : 3	Small	0.4967	SEM
B1	B1-0; B1-5; B1-10; B1-15; B1-20	9.5–16 mm : 26.5–31.5 mm = 1 : 3	Medium	0.5078	Triaxial
B2	B2-0; B2-5; B2-10; B2-15; B2-20	9.5–16 mm : 26.5–31.5 mm = 1 : 3	Medium	0.5078	Triaxial
B3	B3-0; B3-5; B3-10; B3-15; B3-20	9.5–16 mm : 26.5–31.5 mm = 1 : 3	Medium	0.5078	Triaxial
C1	C1-0; C1-5; C1-10; C1-15; C1-20	19–26.5 mm : 31.5–37.5 mm = 1 : 1	Large	0.5171	Triaxial
C2	C2-0; C2-5; C2-10; C2-15; C2-20	19–26.5 mm : 31.5–37.5 mm = 1 : 1	Large	0.5171	Triaxial
C3	C3-0; C3-5; C3-10; C3-15; C3-20	19–26.5 mm : 31.5–37.5 mm = 1 : 1	Large	0.5171	Triaxial
C4	The test specimens chosen from C4	19–26.5 mm : 31.5–37.5 mm = 1 : 1	Large	0.5171	SEM

Note. A1–A3 indicate the large grouted coal-crushed body (Figure 4(a)) with the same grain size mixtures for obtaining the average experimental values in this study; A1-0 to A1-20 mean the small grouted standard cylindrical test specimens (Figure 4(b)) cored from the same grouted coal-crushed body subjected to triaxial compressive strength tests under the confining pressure from 0 to 20 MPa; and the specimens chosen from A4 and C4 were used for SEM tests (not subjected to triaxial compressive strength tests).

Figure 1: Grain size mixture of the crushed coal sample prepared for the grouting tests.

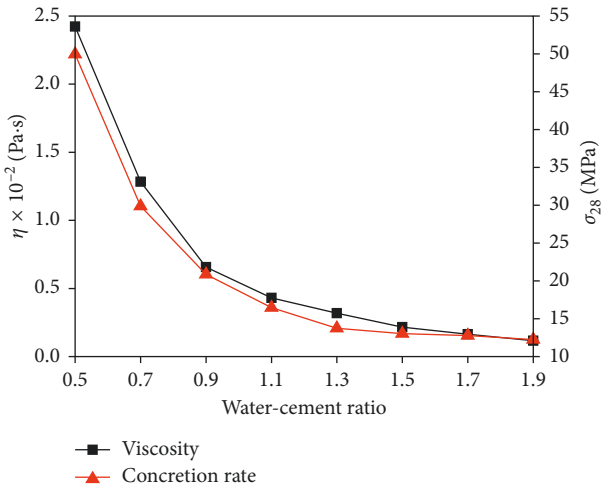

Figure 2: Viscosity and the strength of 28 days of curing for the grouts versus water-cement relationships.

(a)

(b)

Figure 3: Continued.

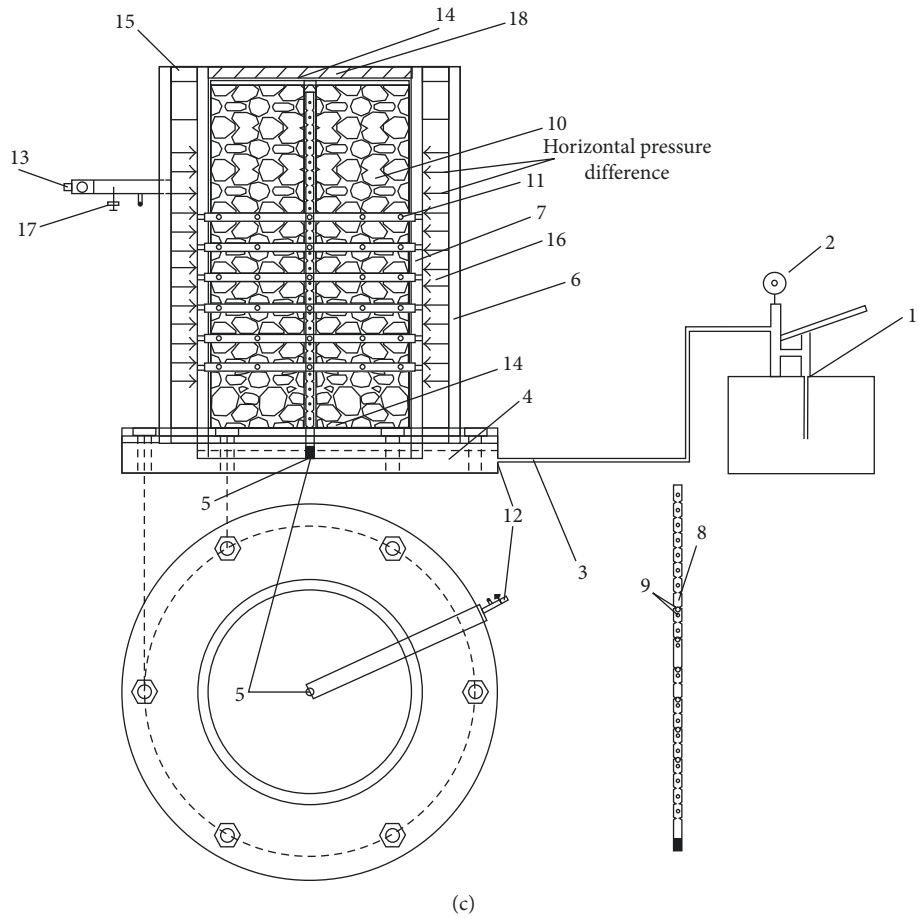

Figure 3: (a) Self-developed grouting experimental apparatus, (b) inner cylindrical grouting barrel used for the placement of the crushed coal sample, and (c) part of the schematic layout of this grouting experimental equipment: 1: controllable grouting pump; 2: pressure gauge; 3: external grouting pipe; 4: bottom plate; 5: grouting hole on the bottom plate; 6: outer grouting barrel; 7: inner grouting barrel; 8: grouting steel tube; 9: small grouting holes on the surface of the grouting steel tube; 10: test specimen; 11: fine holes attached to the sidewall of the inner barrel; 12: bottom valve; 13: outlet; 14: seal rings; 15: sealing plug; 16: channel between the inner and outer barrels; 17: safety valve on the outlet; 18: load-bearing plate.

Figure 2, the water-cement ratio of 0.7 for the grouts (near the approximate turning points on both curves) was chosen in this study, taking improved flow and mechanical characteristics into account at the same time.

2.2. Testing System. Figure 3(a) displays a picture of the self-developed grouting experimental setup, which mainly consists of the grout supply system, grout test system, pipe system, and pressure gauges. Figure 3(b) shows the inner cylindrical grouting barrel used for the placement of the crushed coal specimen. The schematic layout of this experimental equipment is displayed in Figure 3(c). Some important components are described below. A controllable grouting pump (1) with a pressure gauge (2) to adjust the grouting rate is used to inject the cement grouts stored in the storage tank into the crushed coal specimens in the inner cylindrical grouting barrel. A grouting test system is mainly composed of four components including a bottom plate (4), cylindrical grouting barrels (outer and inner barrels) (6 and 7), a grouting steel tube (8), and the load-bearing plate (18). A channel (16) of 35 mm in ring width is left between the inner and outer barrels to induce a horizontal internal and external pressure difference, which can be monitored by the pressure gauge on the outlet (13). This horizontal pressure difference acting on the specimens in the inner barrel through the fine holes (11) attached to the sidewall of the inner barrel is designed to make the grouts permeate and diffuse more sufficiently inside the specimens. Split grouting is likely to occur during grouting due to the greater pressure difference.

2.3. Experimental Procedure and Methods. Two valves (12 and 17) are located at the entrance and exit points of the grouting barrel to adjust the grouts flowing into and out of the specimen, respectively. In detail, during grouting, the bottom valve was opened to allow the grouts to enter the grouting barrel. Meanwhile, the upper valve remained closed during penetration of grouts into the test specimen. As the grouts continually permeated into the specimen under the grouting pressure, the open spaces and small

(a) (b)

Figure 4: (a) Grouting reinforced body (270 mm × 500 mm) from the inner barrel and (b) small grouted standard cylindrical specimens (50 mm × 100 mm) cored from the grouting reinforced body.

Figure 5: MTS 815 rock mechanical test system.

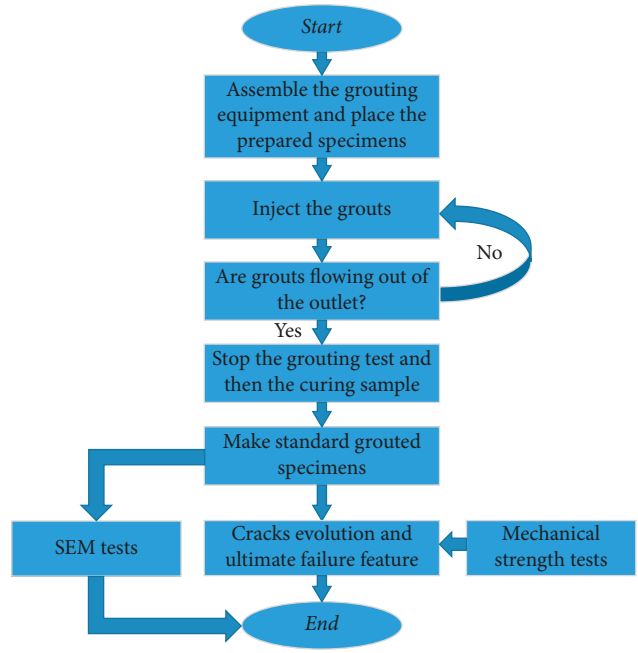

Figure 6: Testing flowchart.

cracks of crushed coal specimens were gradually filled with the grouts. When the pressure difference between the outer and inner barrels reached the designed value, the safety valve (17) opened automatically to release the excess grouts. The grouting devise should be cleaned carefully just after the grouting experiments have been completed. Subsequently, the grouting specimens underwent 28 days of curing under standard conditions, and these prepared grouted specimens were cut into small standard specimens for mechanical testing.

After performing the grouting tests and curing the specimen, more than 45 pieces of small grouted standard cylindrical specimens (e.g., Figure 4(b) and Table 2) with the same height to diameter ratio of 2 (100 mm×50 mm) were extracted from the grouting reinforced body (270 mm × 500 mm) (Figure 4(a)) and were subjected to triaxial compressive strength tests by using the MTS 815 rock mechanical test system (Figure 5). In the strength tests, at first, the axial and the confining pressures were applied at preset values at the loading rate of 0.05 MPa/s. However, in the mechanical tests, the axial displacement loading control mode was used, and then, the axial load was applied again at the loading rate of 0.005 mm/s, while maintaining the prescribed constant confining pressure at the values of 0, 5, 10, 15, and 20 MPa (these values of confining pressure in our research were selected to better simulate the actual stress state in Zhaozhuang mine, Shanxi province, China, where the confining pressure is between 10 and 20 MPa) until the standard grouted test specimen showed damage. Finally, microstructure scanning tests for the specimens chosen from the left 10 pieces of the grouted specimens (A4 and C4) were conducted by SEM.

The flowchart in Figure 6 summarizes the complete test procedure; each of the reported values for the mechanical parameters represents the average value of the three specimens.

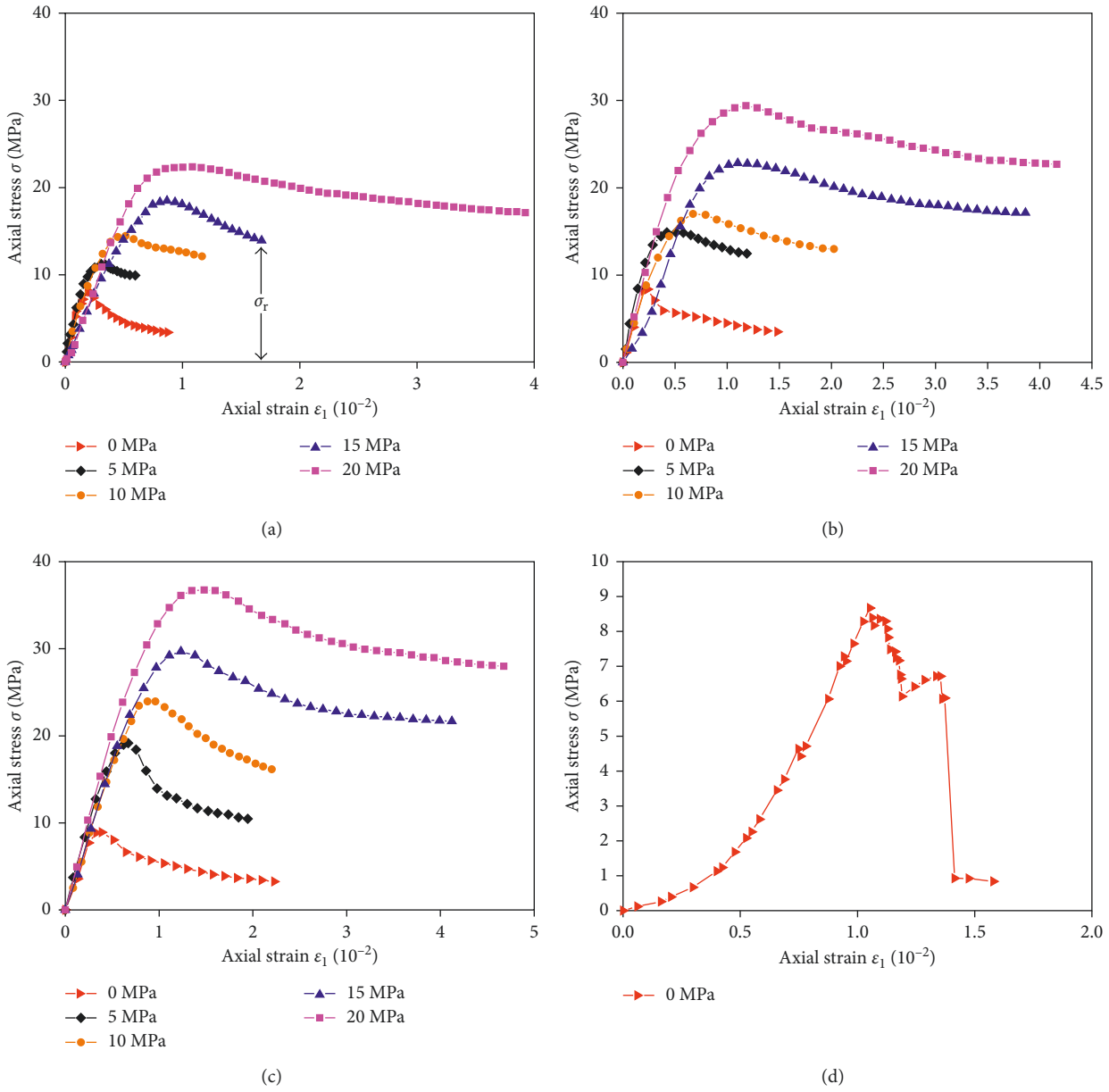

FIGURE 7: Stress-strain curves of grouted crushed coal specimens with different grain size mixtures under different confining pressures. (a) Small specimen, (b) medium specimen, (c) large specimen, and (d) representative original coal specimen.

3. Results and Discussion

3.1. Stress-Strain Relations. The stress-strain curves of the representative triaxial compression tests for the grouted specimens associated with three kinds of grain size distributions under different confining pressures after 28 days of curing are plotted in Figure 7. σ and n represent the axial stress and strain of the grouted specimen, respectively. The triaxial compression stress-strain curves of the grouted specimens have gone through the stages of compaction, elasticity, yield, destruction, softening, and residual stresses. Comparing with the stress-strain curve of the representative original coal specimen (Figure 7(d)), there are no obvious brittle failures in the grouted specimens, because the curves declining moderately after the peak strength, demonstrating that the grouted crushed coal has a good ductility that is conducive to maintaining structural stability when damage occurs.

3.2. Mechanical Parameters. Peak strength (σ_p), residual strength (σ_r), and peak strain (ε_p) are the important parameters reflecting the basic mechanical properties of rocks, particularly of grouted rocks, which are essential for rock mass classification and the development of rock and rock mass failure criteria [22]. Figure 8 illustrates the average values of σ_p, σ_r, and ε_p of the grouted specimens in 3 groups of grain size mixtures versus different confining pressures. Figure 8(a) depicts, for the same grain size mixture, σ_p of grouted specimens that increase with the increase in σ_3, with maximum mean values of 22.38, 29.41, and 36.75 MPa for

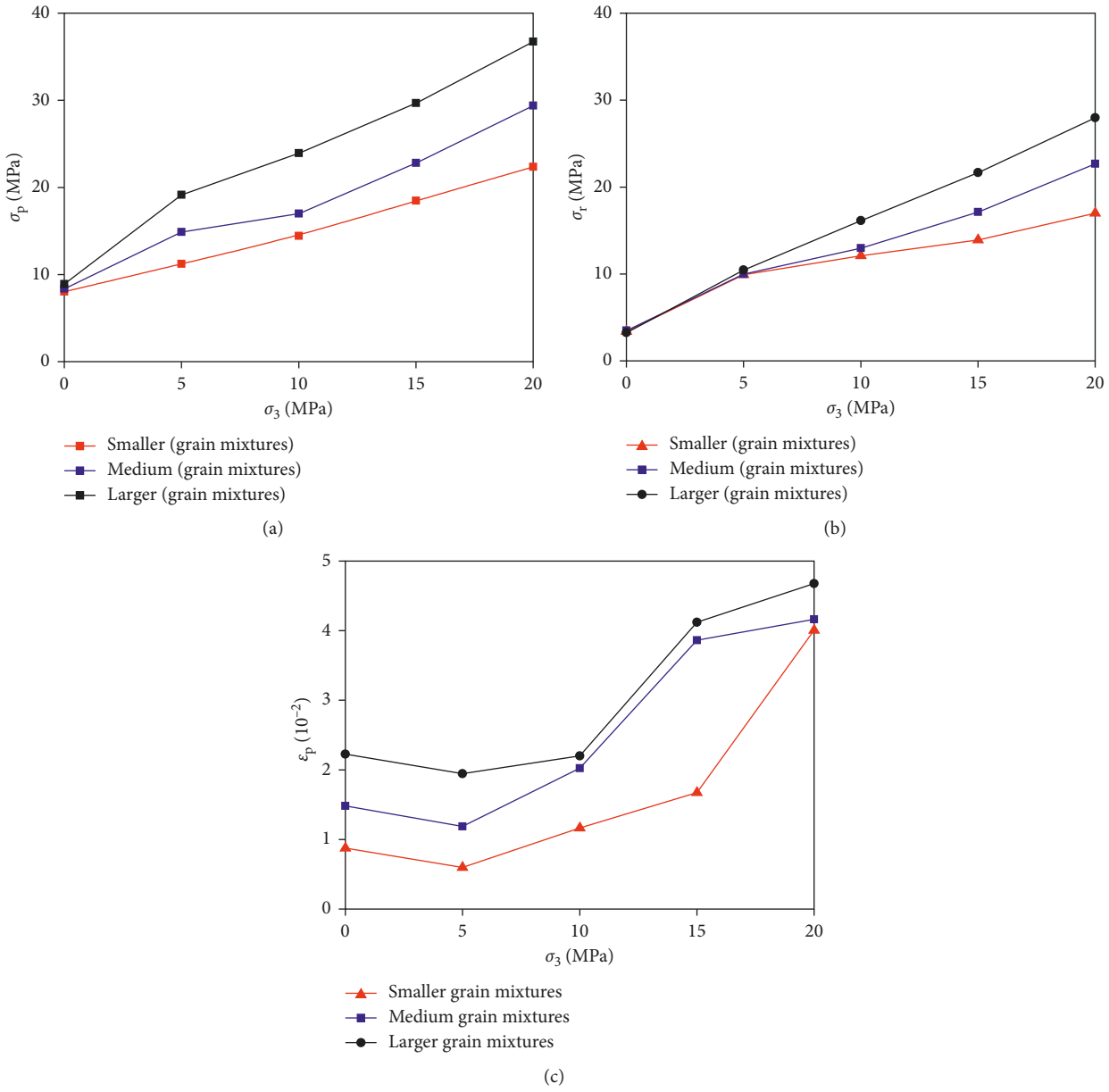

Figure 8: (a) Average values of peak strengths, (b) average values of residual strengths, and (c) average values of peak strains of grouted specimens with different grain size mixtures versus confining pressures.

Table 3: The average slope values of the σ_p-σ_3 and n_r-σ_3 curves

Grain size mixtures	Large	Medium	Small
σ_p-σ_3	1.3241	0.9996	0.7180
σ_r-σ_3	1.2138	0.9103	0.6248

a σ_3 value of 20 MPa. In accordance with the relationship of peak strength and confining pressure, the residual strengths of the grouted specimens were also enhanced with the increasing confining pressure (Figure 8(b)). When σ_3 was 0 to 20 MPa, the values of σ_p and σ_r for the grouted specimens with small grain mixtures increased by approximately 178%, the medium specimens increased by 251%, and the large specimens increased by 312%, which clearly indicated that the grain size distribution and confining pressure had positive effects on improving the mechanical characteristics of the grouted crushed coal. Moreover, the average slope values of the σ_p-σ_3 curves for the grouted specimens of different grain size mixtures were all larger than those of the σ_r-σ_3 curves, and the average slope values of the σ_p-σ_3 and n_r-σ_3 curves are listed in Table 3. This concluded that the confining pressure influence on peak strength is more substantial than that on residual strength in this confining pressure range. Generally, under the confining pressure, the cracks and pores in the grouted specimen are compacted again, resulting in improved mechanical properties of the grouted crushed coal. Similar conclusions in other rock specimens were also confirmed by previous studies [23, 24].

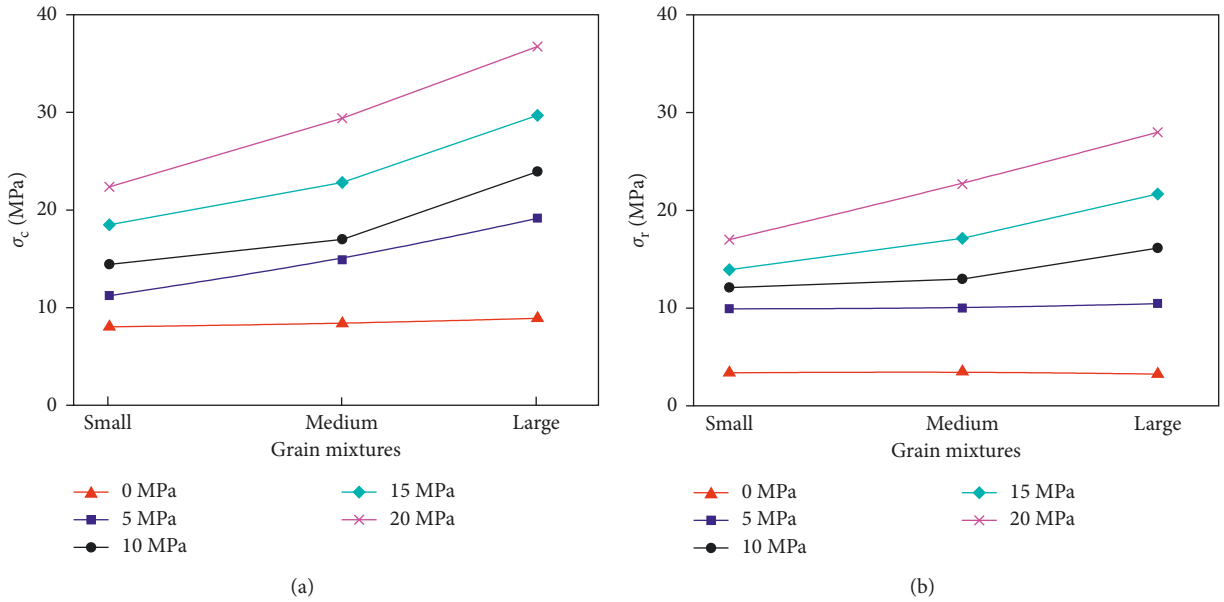

Figure 9: (a) Average values of peak strengths and (b) average values of residual strengths of different confining pressures versus the grouted specimens with different grain size mixtures.

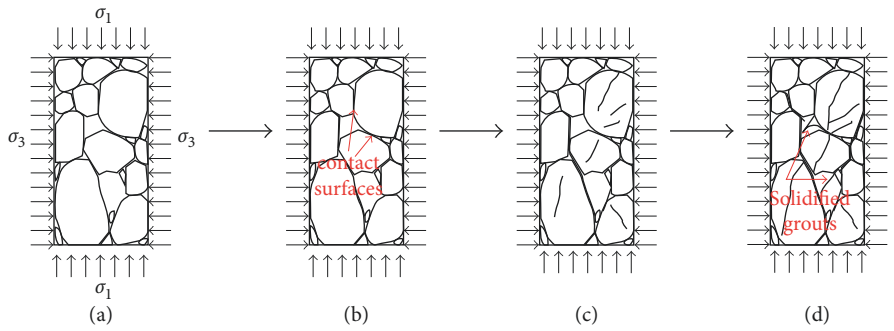

Figure 10: Microscopic cracks evolution process in the grouted crushed coal specimen with the confining pressure being constant and the axial pressure increasing gradually.

A nonlinear increasing trend of the ε_p-σ_3 curves for grouted specimens of different grain size mixtures is observed in Figure 8(c), and comparing the values of ε_p between 0.0087 and 0.022 (at σ_3 of 0 MPa) to those between 0.040 and 0.047 (at σ_3 of 20 MPa) indicates that the ductility and plasticity of the grouted specimen were significantly enhanced when the confining pressure increased. Though ε_p had nearly sustained growth as the confining pressure increased, a slight decrease (<30%) occurred at 5 MPa, which was possibly attributable to the development of confining pressure. In addition, the values of ε_p increased when the grain size distribution (mixtures) was prepared from small to large at the same confining pressure.

On the contrary, σ_p and σ_r were highly affected by different grain size mixtures at the same confining pressure, which both linearly increased as the grain size mixtures varied from small to large, as displayed in Figures 9(a) and 9(b). This is because there are many large coal gravels playing a major role in supporting the external load at a certain stage (the strength of the coal gravel is higher than that of the contact interface between the coal gravels and grouts) when the cracks initiate and propagate within the grouted specimen, as analysed in detail in the next section. Particularly, for the changes in confining pressure from 0 to 20 MPa, the slopes of the peak (or residual) strength curves gradually increased, indicating that the effect of the grain size mixture on the peak (or residual) strength increased at higher confining pressures.

3.3. Crack Evolution Process and the Ultimate Failure Features. To further explain the strong dependence of the mechanical behaviours of the grouted crushed coal specimen on the variation in the grain size mixtures as well as the confining pressure, the possible crack evolution process inside the grouted coal specimen before ultimate failure, with the confining pressure being constant and the axial pressure increasing gradually under triaxial compression, is proposed in Figure 10. The successive damage modes of crack propagation in the grouted specimen during triaxial compression were analysed in detail, including (1) the initial

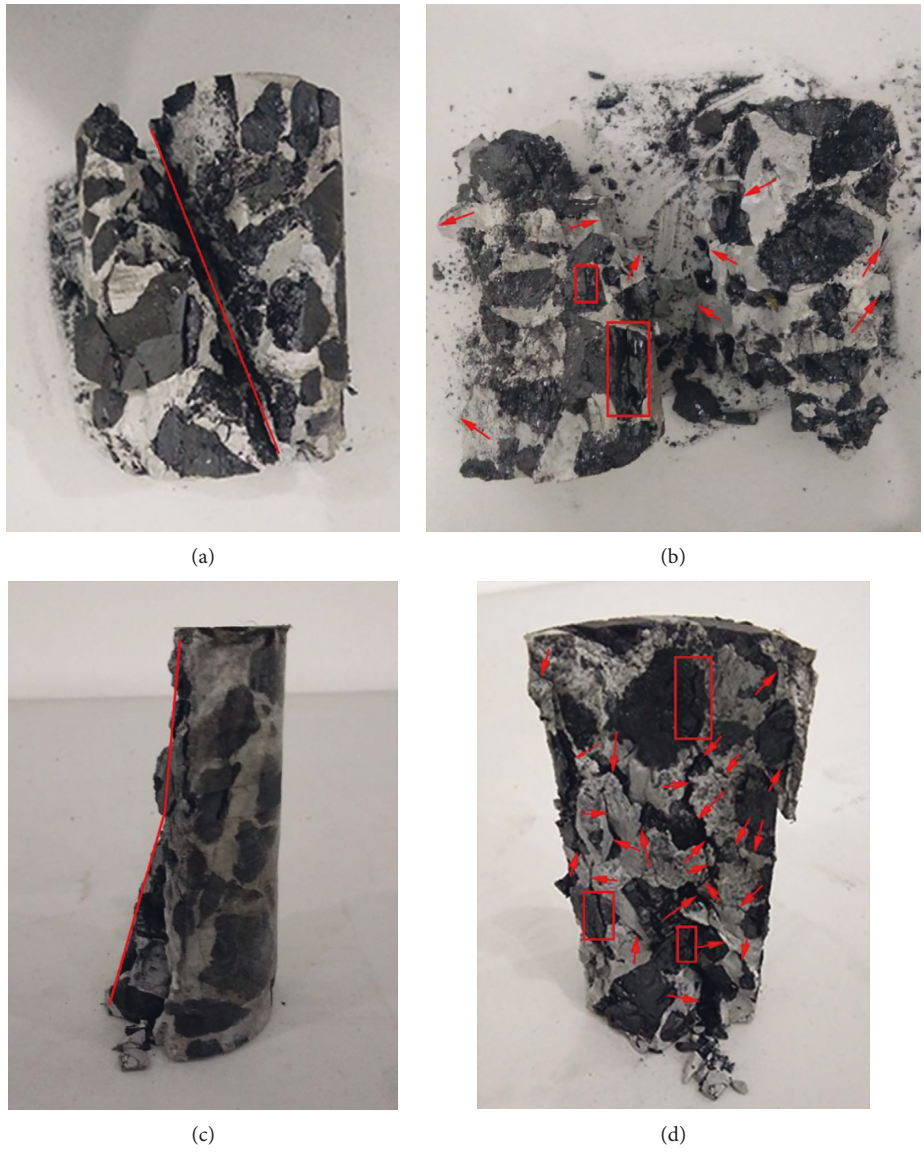

Figure 11: Ultimate failure of the medium specimens under the confining pressure of 5 MPa and 15 MPa, respectively. Fracture profiles: (a) 5 MPa; (c) 15 MPa. Crack distribution: (b) 5 MPa; (d) 15 MPa.

damage to the specimen with the initiation and propagation of cracks along the contact interfaces between the coal gravels and the solidified grouts (Figure 10(b)); (2) the moderate damage with the initiation and propagation of cracks in partial coal gravels (Figure 10(c)); and (3) the serious damage with the further propagation of cracks in the contact interfaces, the partial coal gravels, and the solidified grouts near the coal gravels (Figure 10(d)). The ultimate failure of the grouted specimen occurred after propagation and coalescence of the cracks through the entire grouted specimen. It is worth noting that although the cracks were continuously developing, the fixed confining pressure limited the volume expansion of the grouted specimen, up to a point. As the confining pressure increased, the cracks within the specimen were further compacted, causing the destruction of the specimen to require a higher external force, which explains why the mechanical strength of the grouted specimen increased with increasing confining pressure.

Generally, the cracks start in the region of low strength and end in the region of high strength in the order of contact interfaces, coal gravels, and solidified grouts. The macroscopic mechanical strength is enhanced with increasing grain sizes, showing the strong dependence of the mechanical behaviours of the grouted crushed coal specimen on the variation in the grain size mixtures, which can be reasonably explained as follows: there are many coal gravels with large grain sizes in the medium and large specimens playing a major role in supporting the external load in the second stage of crack propagation (Figure 10(c)), which enhances the ability of the specimen to resist external forces. Moreover, the propagation of the vertical cracks may be suppressed by the confining pressure, so there were more cracks with shear expansion in the grouted specimen.

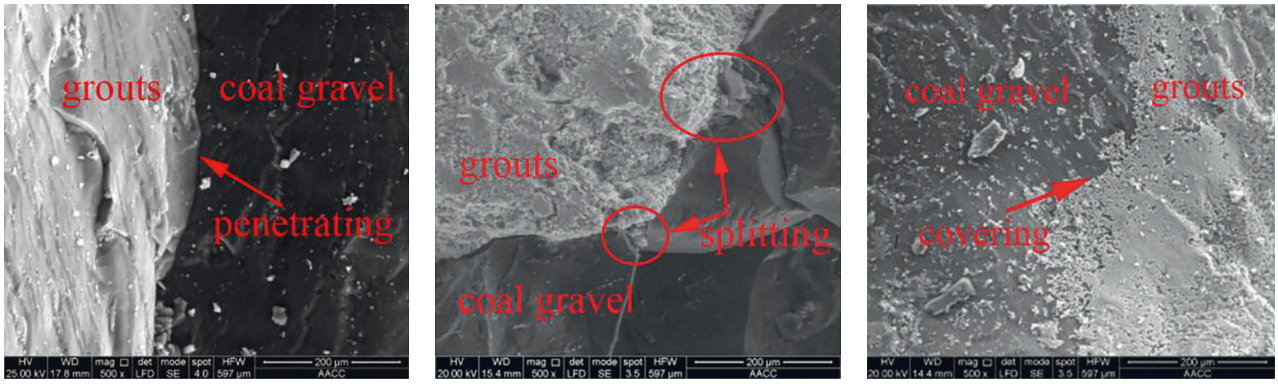

(a) (b) (c)

Figure 12: Three microscopic diffusion modes for the grouts flowing in most of the grouted crushed coal specimens obtained from the SEM images (magnified in the scale of 1 : 500) of failure surfaces. (a) Small specimen: grouts penetrating into the voids around the coal gravels (filling). (b) Large specimen: splitting the coal gravels first and then penetrating into them. (c) Small or large specimen: covering the coal gravels.

After the propagation and coalescence of these cracks within the grouted specimen, the ultimate failure occurred under triaxial compression. With the increase in the confining pressure from 0 to 20 MPa, the ultimate failure modes in most of the grouted crushed coal specimens show a certain regularity: as the confining pressure increases, the internal structural damage characteristics of the grouted specimens after ultimate failure are more obvious and complicated, showing that more cracks were distributed along the contact interfaces between the coal gravels and the solidified grouts. To avoid redundancy, using the grouted specimens under the confining pressures of 5 MPa and 15 MPa as examples (Figure 11, the distribution of the cracks along the contact interfaces is indicated by the red arrows, and the cracks in the coal gravels are marked by the red rectangles), from Figure 11, it is clearly shown that the largest number of observed cracks and damage occurred along the contact interfaces between the coal gravels and the solidified grouts. Additionally, cracks occurred in the partial coal gravels, but the number of cracks in the coal gravels is significantly less than that at the contact interfaces, which seems to be consistent with the evolution mechanism of the cracks in the grouted coal specimen presented above: the contact interfaces are the most vulnerable parts within the grouted specimen for supporting the external load, and more cracks are easily formed in this part of the specimen. Moreover, the fracture profiles that occurred in most of the grouted specimens are dominated by shear failure, as shown in Figure 11.

3.4. Microscopic Cementation Features. The observed improvement in the mechanical characteristics of the grouted crushed coal can be further analysed by SEM. Micrographs of parts of the failure interfaces of representative grouted specimens (not subjected to the triaxial compressive tests) magnified at the scale of 1 : 500 are shown in Figure 12. There may be three main microscopic diffusion modes for the grouts flowing in most of the crushed coal specimens with different grain mixtures: grouts penetrating the large voids around the coal gravels (Figure 12(a)), grouts splitting the partial coal gravels to form voids and then penetrating the voids (Figure 12(b)), and grouts covering the coal gravels (Figure 12(c)), which can result in different microscopic cementation features such as contact bonding, wedge action, and interface adhesion bonding, respectively. For example, as shown in Figure 12(a), the voids around the coal gravels (black part) were permeated and tightly infilled with cement grouts (white part), which act as adhesive ties to the coal gravels, together forming a dense, impermeable, high-strength structure mainly in the specimens with small grain mixtures. However, among most of the specimens with large grain mixtures, there were microscopic splitting cracks occurring in the coal gravels, indicating that splitting grouting occurred in the coal gravels, as shown in Figure 12(b), and as a result, the macroscopic strength of the grouted specimen with large grain mixtures appeared to be affected by the splitting grouting and, thus, presented a larger value (as shown in Figure 8, the reason may be attributed to the grouts splitting and entering the coal gravels, which produced certain "wedge actions" that increased the strength of the grouted specimen). This splitting phenomenon was mainly due to the greater pressure difference between the inner and outer barrels, as analysed in Testing System. Generally, different diffusion modes for the grouts flowing in the crushed coal would result in different reinforcement effects in the grouted specimens, among which the splitting grouting mode on the reinforcement effect for the grouted specimen seems to be better than that of the penetrating (filling) grout, on the basis of the detailed analysis above. The explanation and contrast of the microstructures in the grouted specimens illustrated that there were at least three types of grout diffusion modes, together forming the skeleton effect among the grouted crushed coal specimens, which leads to a satisfactory grouting reinforcement effect.

4. Discussion

The mechanical properties of the grouted crushed coal are difficult to describe accurately due to the influence of the grouting parameters and the cementation characteristics

between the two different materials (rock and grout). Further study is necessary to improve the quality of this work. For example, some mathematical analysis or fitting model should be presented, and the "fractal dimension" should also be used to reasonably describe the breaking degree and grain size distribution of the coal [25].

In spite of this, the findings from this study have some engineering implications, and it is found that the appropriate confining pressure is favourable for the improvement in the strength of the grouted crushed coal, which is similar to the other ungrouted rock mass [23, 24]. This study also indicates that the grain size mixtures of the crushed coal have important implications on the mechanical behaviours of the grouted crushed coal, suggesting that the grouting parameters can be adjusted accordingly (e.g., properly reducing the amount of grout in the crushed area with large grain mixtures is reasonable because of the mechanical properties of the grouted specimen with large grain mixtures being better). Moreover, the crack evolution mechanism and the ultimate failure feature of the grouted crushed coal suggest that there is a defect in the cohesive force of the contact interfaces between the grouts and coal gravels, which causes the contact interfaces to be the most vulnerable parts of the grouted specimen for supporting the external load. Hence, more effective grouting materials need to be developed to account for this vulnerability.

5. Conclusions

A series of tests using an in-house developed grouting apparatus were conducted to study the influence of grain size mixtures and stress state on the mechanical behaviours of the grouted crushed coal specimens. The following conclusions can be made: the peak (σ_p) and residual (σ_r) strengths of the grouted specimens with the same grain size mixture are highly related to the confining pressure. σ_p and σ_r increase with increasing σ_3. The average slope values of the σ_p-σ_3 curves for the grouted specimens with different grain size distributions are all larger than those of the σ_r-σ_3 curves, which demonstrates that the confining pressure has more significant effects on the peak strength than on the residual strength. The ε_p-σ_3 plots for the grouted specimens of different grain size mixtures display a nonlinear increasing trend with increasing confining pressure. This is mainly because the ductility and plasticity of the grouted specimen are significantly enhanced when the confining pressure increases. For a constant confining pressure, the peak and residual strengths of the grouted specimens both gradually increase approximately linearly, while the grain size mixtures vary from small to large, but the peak (or residual) strengths are highly affected by the grain size mixture at higher confining pressures. A possible successive evolution process is proposed for the internal cracks that occur during deformation of the grouted specimen under triaxial compression, including three main stages, as follows: (1) initiation and propagation of cracks along the contact interfaces between the coal gravels and solidified grouts; (2) initiation and propagation of cracks in partial coal gravels; and (3) further propagation of cracks at the contact interfaces, the local coal gravels, and then, the solidified grouts near the local gravels. Subsequently, the ultimate failure of the grouted specimen, characterized by the fracture profiles of shear failure and the occurrence of more cracks at the contact interfaces, occurred after the propagation and coalescence of the cracks through the entire specimen. Moreover, there are three major microscopic diffusion modes for the grouts flowing in most of the crushed coal specimens. The three microscopic diffusion modes of grouts lead to different microscopic cementation features including contact bonding, wedge action, and interface adhesion bonding, respectively. The mechanical properties of the large specimen are the best, which seem to indicate that the reinforcement effect of the grouted specimen related to the splitting grouting mode is substantial.

Symbols

σ: Axial stress (MPa)
ε_1: Axial strain (10^{-2})
σ_p: Peak strength (MPa)
σ_r: Residual strength (MPa)
σ_3: Confining pressure
ε_p: Peak strain (10^{-2})
SEM: Scanning electron microscopy.

Conflicts of Interest

The authors declare that there are no conflicts of interest regarding the publication of this paper.

Acknowledgments

This research was financially supported by the National Natural Science Foundation of China (Grant nos. 51704280 and 51574223) and the China Postdoctoral Science Foundation (Grant no. 2017T100420). Haizhi Zang would like to thank the financial support provided by State Key Laboratory for Geomechanics and Deep Underground Engineering, China University of Mining and Technology (SKLGDUEK1805), and Research Fund of State Key Laboratory of Coal Resources and Safe Mining, CUMT (SKLCRSM18KF024).

References

[1] S. W. Lee, J. Minki, K. Ji-Whan, and T. Kim, "Application of Ca-doped mesoporous silica to well-grouting cement for enhancement of self-healing capacity," *Materials and Design*, vol. 89, pp. 362–368, 2016.

[2] J. Liu, J. Song, Z. Zhang, and N. Hu, "Influence of the ground displacement and deformation of soil around a tunnel caused by shield backfilled grouting during construction," *Journal of Performance of Constructed Facilities*, vol. 31, no. 3, p. 04016117, 2017.

[3] J. M. Minto, E. Maclachlan, G. E. Mountassir, and R. J. Lunn, "Rock fracture grouting with microbially induced carbonate precipitation," *Water Resources Research*, vol. 52, no. 11, pp. 8827–8844, 2016.

[4] M. H. Mohammed, R. Pusch, and S. Knutsson, "Study of cement-grout penetration into fractures under static and oscillatory conditions," *Tunnelling and Underground Space*

Technology Incorporating Trenchless Technology Research, vol. 45, pp. 10–19, 2015.

[5] M. Mollamahmutoğlu and E. Avci, "Ultrafine Portland cement grouting performance with or without additives," *KSCE Journal of Civil Engineering*, vol. 19, no. 7, pp. 2041–2050, 2014.

[6] M. E. Tani, "Grouting rock fractures with cement grout," *Rock Mechanics and Rock Engineering*, vol. 45, no. 4, pp. 547–561, 2012.

[7] J. Funehag and Å. Fransson, "Sealing narrow fractures with a Newtonian fluid: model prediction for grouting verified by field study," *Tunnelling and Underground Space Technology*, vol. 21, no. 5, pp. 492–498, 2006.

[8] W. Sui, J. Liu, W. Hu, J. Qi, and K. Zhan, "Experimental investigation on sealing efficiency of chemical grouting in rock fracture with flowing water," *Tunnelling and Underground Space Technology incorporating Trenchless Technology Research*, vol. 50, no. 1, pp. 239–249, 2015.

[9] K. Yoneyama, T. Okuno, A. Nakaya, and H. Tosaka, "Experimental and numerical study on fracture grouting by fine particle cement," *Chemistry Letters*, vol. 1994, no. 1, pp. 9–12, 2012.

[10] D. Ma, Q. Li, M. Hall, and Y. Wu, "Experimental investigation of stress rate and grain size on gas seepage characteristics of granular coal," *Energies*, vol. 10, no. 4, p. 527, 2017.

[11] Q. Wu, S. Xu, W. Zhou, and J. Lamoreaux, "Hydrogeology and design of groundwater heat pump systems," *Environmental Earth Sciences*, vol. 73, no. 7, pp. 3683–3695, 2015.

[12] Z. Zhou, X. Cai, D. Ma, W. Cao, L. Chen, and J. Zhou, "Effects of water content on fracture and mechanical behavior of sandstone with a low clay mineral content," *Engineering Fracture Mechanics*, vol. 193, pp. 47–65, 2018.

[13] J. Shu, X. Ren, J. Zhang, and H. Ren, "Influence mechanism of grouting on mechanical characteristics of rock mass," *Mathematical Problems in Engineering*, vol. 2013 Article ID 281817, 6 pages, 2009.

[14] J. Zhou, Y. Liu, C. Du, and F. Wang, "Experimental study on crushing characteristic of coal and gangue under impact load," *International Journal of Coal Preparation and Utilization*, vol. 36, no. 5, pp. 272–282, 2015.

[15] I. Engelhardt and S. Finsterle, "Thermal-hydraulic experiments with bentonite/crushed rock mixtures and estimation of effective parameters by inverse modeling," *Applied Clay Science*, vol. 23, no. 1, pp. 111–120, 2003.

[16] G. Guida, M. Bartoli, F. Casini, and G. M. B. Viggiani, "Weibull distribution to describe grading evolution of materials with crushable grains," *Procedia Engineering*, vol. 158, pp. 75–80, 2016.

[17] J. Legrand, "Revisited analysis of pressure drop in flow through crushed rocks," *Journal of Hydraulic Engineering*, vol. 128, no. 11, pp. 1027–1031, 2002.

[18] D. Ma, M. Rezania, H. S. Yu, and H. B. Bai, "Variations of hydraulic properties of granular sandstones during water inrush: effect of small particle migration," *Engineering Geology*, vol. 217, pp. 61–70, 2017.

[19] J. Liu, J. Wang, Z. Chen, S. Wang, D. Elsworth, and Y. Jiang, "Impact of transition from local swelling to macro swelling on the evolution of coal permeability," *International Journal of Coal Geology*, vol. 88, no. 1, pp. 31–40, 2011.

[20] D. Ma, Z. Zhou, J. Wu, Q. Li, and H. Bai, "Grain size distribution effect on the hydraulic properties of disintegrated coal mixtures," *Energies*, vol. 10, no. 5, p. 612, 2017.

[21] D. Ma, X. Cai, Z. Zhou, and X. Li, "Experimental investigation on hydraulic properties of granular sandstone and mudstone mixtures," *Geofluids*, Article ID 9216578, 2018, In press.

[22] J. C. Jaeger and N. G. W. Cook, *Fundamentals of Rock Mechanics*, Chapman and Hall, London, UK, 3rd edition, 1979.

[23] K. Hashiba and K. Fukui, "New multi-stage triaxial compression test to investigate the loading-rate dependence of rock strength," *Geotechnical Testing Journal*, vol. 37, no. 6, p. 20140061, 2014.

[24] S. Q. Yang, "Strength and deformation behavior of red sandstone under multi-stage triaxial compression," *Canadian Geotechnical Journal*, vol. 49, no. 6, pp. 694–709, 2012.

[25] W. Wei and Y. Xia, "Geometrical, fractal and hydraulic properties of fractured reservoirs: a mini-review," *Advances in Geo-Energy Research*, vol. 1, no. 1, pp. 31–38, 2017.